Journal of Intelligent & Robotic Systems (2022) 106:75
https://doi.org/10.1007/s10846-022-01768-0

SHORT PAPER

Mathematical Modeling and Stability Analysis of an Effective Design of Biomimetic AUV

M. V. Aruna[1]

Received: 23 August 2022 / Accepted: 7 November 2022 / Published online: 12 December 2022

Abstract
The research on autonomous underwater vehicles (AUVs) has accomplished enormous attention during the last few decades because of its applications in many marine systems fields. A significant number of AUVs have been developed to solve the wide range of scientific and applied tasks of ocean research and development worldwide. Thus the main aim of this research is to provide an effective mathematical model of Biomimetic AUV dynamics. For instance, to develop high-fidelity AUV simulation and control algorithms, we need to know the overall mathematical model of AUV dynamics. In order to endorse the ability of the proposed model, stability analysis has been performed, and the model is validated by designing a coupled velocity tracking control using a PID controller.

Keywords Mathematical model · Dynamics · AUV · PID control

1 Introduction

Autonomous underwater vehicles are robots that operate without the intervention of human beings. In the last few decades, a large amount of research has been conducted in this area due to its applications in numerous marine systems domains. Since the beginning of civilization, nature has inspired the human imagination. Evolution has fine-tuned the features of living organisms over millions of years to perform tasks with extraordinary [1] efficiency. Thus an advancement in the underwater vehicle study is focused on biomimetic or biologically inspired AUVs.

The first AUV was evolved by the Applied Physics Laboratory of the University of Washington by Stan Murphy, Bob Francois in 1957, and later Terry Ewart. This "Special Purpose Underwater Research Vehicle" or SPURV [2] was utilized to investigate diffusion, acoustic transmission, and undersea [3] wakes. Other early AUVs were created in the 1970s at the Massachusetts Institute of Technology [3]. The biomimetic propulsion system is a well-suited alternative to conventional propeller system. The well known biomimetic AUVs are Robo tuna, Robo pike, Essex robotic fish, Bio swimmers, Robo slamon, Vorticity Controlled Unmanned Underwater vehicle etc.

At the request of the United States Navy, Gertler published the standard equations of motion for submarines in [4] in 1967. Feldman subsequently refined these equations in 1979 [5]. Due to the comprehensive treatment of hydrodynamic coefficients [6], the standard equations of motion for submarines are incredibly accurate. The inherent nature of human-crewed submarines necessitates such precise models and state-of-the-art hydrodynamic modeling, particularly regarding test facilities and personnel. AUV development costs are not comparable to human-operated submarines [6]. In contrast to submarines, AUVs operate autonomously, making robust and precise control essential. In this context, evaluating the mathematical modeling and stability analysis of the AUVs is of the utmost importance. The most popular methods for modeling AUVs are Humphrey's [7], Nahon's [8] and Fossen's [9, 10] models.

Statement of Contributions The present work contributes a practical design of the virtual model of Biomimetic AUV, which mimics a fish. The vehicle consists of a Gertler geometric shaped hull, caudal fin-like tail, pectoral fins, and dorsal fins [11] like a fish. The dynamic model of each part of the vehicle has been taken and coupled with appropriate methods to get an adequate model. The stability analysis has been performed to check the control quality of the proposed

✉ M. V. Aruna
arunodayam92@gmail.com

[1] Department of Ocean Engineering, Indian Institute of Technology, Madras, Adayar, Chennai, 600036, Tamilnadu, India

system. A PID controller with genetic algorithm tuning is implemented for the velocity tracking, roll and pitch control applications with the presence of disturbance cases (ocean current and wave disturbance) for the coupled biomimetic AUV system to substantiate the vehicle behavior. In order to check the capability of the vehicle, a stress assessment method is also added.

This paper is organized into seven sections. In Section 2, the description of the proposed Biomimetic AUV model is presented. The complete mathematical modeling and representation of AUV system is explained in Section 3. In Section 4, stability analysis of the coupled system has been performed, and Section 5 illustrates the stress assessment of the system. Coupled vehicle system control for different tracking systems are explained in Section 6. The stability analysis outcomes with coupled velocity, roll and pitch control system responses are explained in Section 7, results and discussion, and the conclusions based on the obtained results are followed in Section 8.

2 System Description

The Biomimetic AUV model used in this research consists of a Gertler geometric shaped hull [12] with a caudal fin which is fitted at the back side of the body, a pair of horizontally mounted pectoral fins and a pair of vertically connected dorsal fins as shown in Fig. 1. The caudal fin can produce the required thrust for the forward/surge motion of the vehicle.

The four fundamental forces acting on an underwater vehicle are thrust (τ), drag (D), lift (L) and weight (W). The force that moves an AUV in the forward direction is called thrust, and it is produced by the caudal fin of the vehicle. Suppose a fluid flowing around an object exerts a force on it. The part of this force perpendicular to the direction of the incoming flow is called lift. In contrast, the drag force, or portion of the force parallel to the flow direction, is the opposite. Weight is the downward force acting on the underwater vehicle. The vehicle responds to

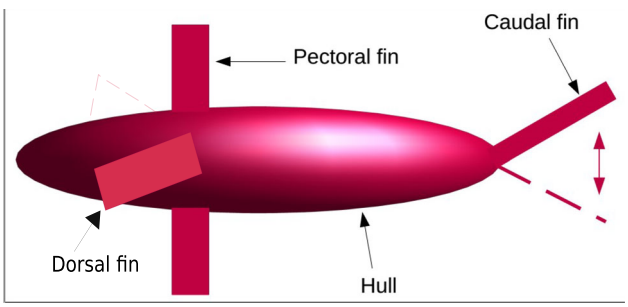

Fig. 1 Pictorial representation of proposed Biomimetic AUV model

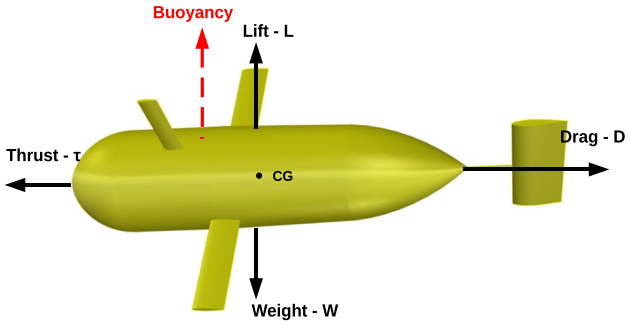

Fig. 2 Proposed biomimetic AUV model with fundamental forces

the entire weight force (W) as if it were focused at the center of gravity or the balancing point (G). The combined force of all hydro-static pressures acting on the hull is buoyancy. All these forces are plays an important role in the analysis of proposed underwater vehicle. Figure 2 illustrates all these forces of the proposed biomimetic AUV.

The hull geometry of the vehicle is Gertler 4154 shaped, [12, 13] and it is possible to add modules at the mid section for batteries or other equipment [12, 14] (Fig. 3).

All the hydrodynamic coefficients are determined using commercial CFD package STAR-CCM+ (PMM test) and the total drag produced by the bare hull is $26.14N$ [15]. The optimum length to diameter (L/D ratio) is an essential parameter for an AUV to get an efficient hydrodynamic structure for underwater vehicles. In the proposed AUV, the length and diameter were chosen ($L/D = 4$) in such a way that the drag is very low. The Fig. 4 shows the L/D ratio vs drag plot of the biomimetic AUV.

It is clear from the first plot, Fig. 4 that the chosen L/D ratio is optimum for the underwater vehicle. Similarly, buoyancy also an important parameter which depends on the L/D ratio. The Fig. 5 illustrates the changes in the L/D ratio with magnitude of buoyant force for the gertler geometric shaped (Gertler 4154) underwater vehicle.

The L/D ratio vs buoyant force plot, states that the magnitude of buoyant force is increases for the changes in L/D ratio. In the current biomimetic AUV model, a depth controller is developed [16] to maintain the AUV at a particular depth using H_∞ controller [16], which indirectly controls the buoyancy [16] of the vehicle. The design parameters of the hull is given in Table 1.

Since the all the foils are undergo lateral and rotational motion, and motors are used to actuate [17] the foil system.

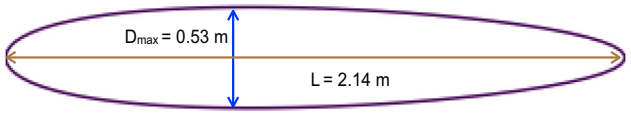

Fig. 3 Representation of basic Gertler geometric profile [12]

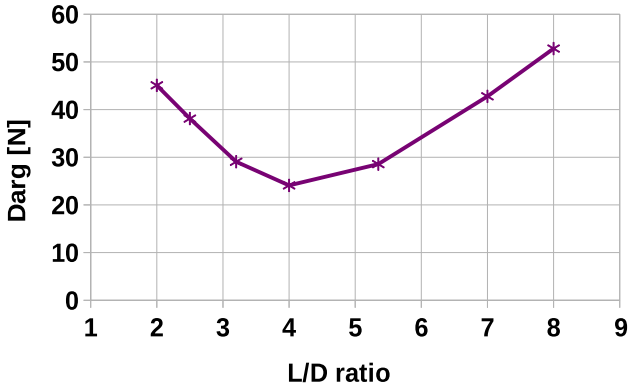

Fig. 4 L/D ratio vs drag plot (Gertler 4154 profile)

The caudal fin undergoes forward (lateral) and rotational motion (roll), so that it can produce the required thrust for the vehicle movement. The roll position of the foil [18] is defined as,

$$\phi(t) = \phi_0 cos(\omega t) \tag{1}$$

where ϕ_0 is the roll amplitude in radians, and ω is the frequency of the foil motion [18] in radians per second. The maximum thrust produced by the caudal fin is $\tau_X = 100N$ with a propulsive efficiency of 78.74% [15].

The pectoral fin undergo heave and pitch motion [18], described as;

$$\begin{aligned} h(t) &= h_0 sin(\omega_h t) \\ p(t) &= p_0 sin(\omega_p t + a) \end{aligned} \tag{2}$$

where: h_0 and p_0 corresponds to the heave amplitude and pitch angle, a is the phase difference between the heaving and pitching motions, and ω_h is the flapping frequency. The

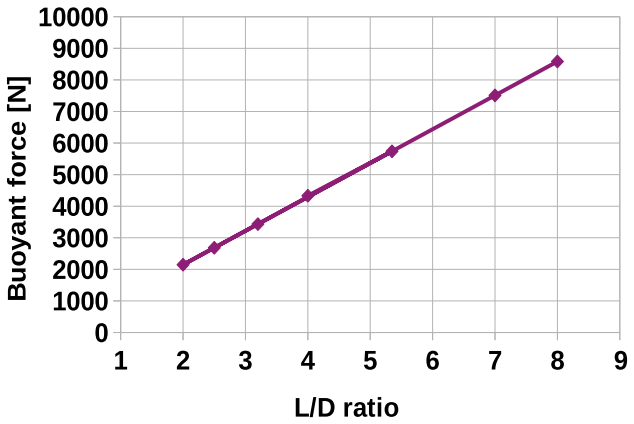

Fig. 5 L/D ratio vs magnitude of buoyant force for AUV (Gertler 4154 profile)

Table 1 Design parameters of the vehicle hull

Design parameters of hull	
Length (m)	2.14
Major Diameter (m)	0.53
Design speed (m/s)	2.57

value of a is $pi/2$ in all experiments. Therefore the heave equation will be,

$$h(t) = h_0 cos(\omega_h t) \tag{3}$$

In the similar way dorsal fin undergo sway-yaw motion, described as:

$$\begin{aligned} s(t) &= s_0 sin(\omega_s t) \\ y(t) &= y_0 sin(\omega_s t + a) \end{aligned} \tag{4}$$

where where s_0 and y_0 correspond to the sway and yaw angle of the pectoral fin,a is the phase difference between the yawing and swaying motions, [29] and ω_s is the flapping frequency. The angle a is taken as $\pi/2$ in all experiments, thus:

$$y(t) = y_0 cos(\omega_s t) \tag{5}$$

The foil NACA63-015A is taken for all the fin models.

3 Mathematical Modeling of Biomimetic AUV System

The coupled mathematical modeling of proposed AUV includes the following such as dynamic modeling of hull and fins.

3.1 Hull Dynamics

The dynamics of the main hull or body of the biomimetic vehicle are modeled by using well-known theories of Fossen [9, 10]. A six-degrees-of-freedom (6DOF) marine vehicle has independent linear and angular motions. Generally, it is used to determine the position and orientation of the vehicle. Linear motions of the system are surge, sway, heave, and angular motions are roll, pitch, yaw. Two coordinate frames are used to describe or analyze the motion of the vehicle, which are Earth fixed frame and body-fixed [10] frame. A body-fixed frame is a moving frame fixed with the vehicle [10]. The general motion of AUV can be given for a system by SNAME (1950) in which η is the position and orientation vector concerning Earth fixed frame,ν is the linear, and angular velocity coordinates concerning body-fixed frame

[9, 10], $g(\eta)$ is the gravitational and buoyancy matrix, and τ is the thrust generated [9, 10] for body-fixed frame.

$$\begin{aligned}\eta &= \begin{bmatrix}\eta_1 & \eta_2\end{bmatrix} = \begin{bmatrix}x & y & z & \phi & \psi & \theta\end{bmatrix}^T \\ V &= \begin{bmatrix}v_1 & v_2\end{bmatrix} = \begin{bmatrix}u & v & w & p & q & r\end{bmatrix}^T \\ \tau &= \begin{bmatrix}\tau_1 & \tau_2\end{bmatrix} = \begin{bmatrix}\tau_X & \tau_Y & \tau_Z & \tau_K & \tau_M & \tau_N\end{bmatrix}^T\end{aligned} \tag{6}$$

The dynamic model of the vehicle on the horizontal plane is as given below:

$$M\dot{v} + C(v)v + D(v)v + g(\eta) = \tau \tag{7}$$

where, M is the inertia matrix, C(v) is the Coriolis and centripetal matrix, D(v) is the damping matrix and τ-input vector [9–11]. The above equation is is derived from the Newton-Euler equation of a rigid body in fluid.

$$\tau = \begin{bmatrix}\tau_X \\ \tau_Y \\ \tau_Z \\ \tau_K \\ \tau_M \\ \tau_N\end{bmatrix} \tag{8}$$

From the dynamic Eq. 7,

$$\dot{v} = M^{-1}[-C(v) - D(v)]v + M^{-1}\tau \tag{9}$$

Let $A = M^{-1}[-C(v) - D(v)]$ and $B = M^{-1}$. Hence the Eq. 9 will be

$$\dot{v} = Av + B\tau \tag{10}$$

and

$$y = Cv \tag{11}$$

where $\dot{v} = \begin{bmatrix}\dot{u} & \dot{v} & \dot{w} & \dot{p} & \dot{q} & \dot{r}\end{bmatrix}^T$ and $v = \begin{bmatrix}u & v & w & p & q & r\end{bmatrix}^T$ is the state space representation of the vehicle hull system.

3.1.1 Surge and roll hull Subsystem Dynamics

The caudal fin is connected series/cascade to the hull subsystem of AUV, in which forward motion dynamic equation explained as:

$$\begin{bmatrix}m - X_{\dot{u}} & 0 \\ 0 & I_x - K_{\dot{p}}\end{bmatrix}\begin{bmatrix}\dot{u} \\ \dot{p}\end{bmatrix} + \begin{bmatrix}-X_u & 0 \\ 0 & -M_p\end{bmatrix}\begin{bmatrix}u \\ p\end{bmatrix} = \begin{bmatrix}\tau_X \\ \tau_K\end{bmatrix} \tag{12}$$

From Eq. 12 equation,

$$\begin{aligned}\begin{bmatrix}\dot{u} \\ \dot{p}\end{bmatrix} = &-\begin{bmatrix}m - X_{\dot{u}} & 0 \\ 0 & I_x - K_{\dot{p}}\end{bmatrix}^{-1}\begin{bmatrix}-X_u & 0 \\ 0 & -M_p\end{bmatrix}\begin{bmatrix}u \\ p\end{bmatrix} \\ &+\begin{bmatrix}m - X_{\dot{u}} & 0 \\ 0 & I_x - K_{\dot{p}}\end{bmatrix}^{-1}\begin{bmatrix}\tau_X \\ \tau_K\end{bmatrix}\end{aligned} \tag{13}$$

The Eq. 13 of the form ;

$$\dot{\hat{u}} = A\hat{u} + B\tau \tag{14}$$

and

$$y = C\hat{u} \tag{15}$$

where $\dot{\hat{u}} = \begin{bmatrix}\dot{u} & \dot{p}\end{bmatrix}^T$ and $\hat{u} = \begin{bmatrix}u & p\end{bmatrix}^T$ is the state space representation of the vehicle forward motion hull system.

3.2 Caudal fin Dynamics

The approach is inspired and borrowed by Lighthill [19]. Lighthill has modeled the thunniform tail, which produces lateral and rotational motions. This approach is based on von Karman model [20–23]. The forces and moments produced by the foils are complicated, which is derived by using unsteady aerodynamic theory [24, 25]. The proposed system is a motor-driven oscillating foil system. It experiences lateral displacement angular rotation. Theodorsen [21, 25] derived the expression for the moment and lift, which act on the foil at the constant velocity free-stream where the foil is harmonically oscillating. Let F_a and τ_a are the driving force and torque applied, and L and M are the hydrodynamic lift and moment acting on the foil [26], respectively. According to the unsteady aerodynamic theory [24],

$$m(\ddot{Z} + \ddot{\alpha}b) = L + F_a \tag{16}$$

where Z is the vertical position and m is the mass.

$$J\ddot{\alpha} = M + \tau_a - F_a b \tag{17}$$

where α is the angular position (pitch angle), J is the moment of inertia and b is the position of axis of rotation [27] along the chord. A complete derivation of lift and moment [27]. A complete derivation of lift and moment has been done by Harper et al. [26] including added mass, wake effect, quasi-steady lift and moment, and thrust and drag based on unsteady aerodynamic theory [25]. Therefore;

$$\begin{aligned}L = &\ 2\pi\rho aU(-\dot{Z} + U\alpha + (\frac{a}{2} - b)\alpha)C(i\omega) \\ &+\pi\rho a^2(-\ddot{Z} + U\dot{\alpha} - b\ddot{\alpha})\end{aligned} \tag{18}$$

$$\begin{aligned}M = &-2\pi\rho aU\left(\frac{a}{2}\right)^2\dot{\alpha} + \pi\rho a^2 U \\ &\times\Big(-\dot{Z} + U\alpha + \Big(\frac{a}{2} - b\Big)\dot{\alpha}\Big)C(i\omega) - \frac{\pi}{8}\rho a^4\ddot{\alpha}\end{aligned} \tag{19}$$

where a is half chord length of tail, ρ is density, U is free stream velocity and $C(i\omega)$ is Theodorsen function

[25]. A third order transfer function obtained for the good approximation of Theodorsen function [25], in this study is

$$C(i\omega) = \frac{a_3(i\sigma)^3 + a_2(i\sigma)^2 + a_1(i\sigma) + a_0}{(i\sigma)^3 + b_2(i\sigma)^2 + b_1(i\sigma) + b_0} \tag{20}$$

where $\sigma = \frac{\omega a}{U}$ which is a non dimensional reduced frequency.

State-space representation of the caudal fin system

Consider the dynamic equations of the fin Eqs. 16 and 17. Substitute the lift and moment Eqs. 18, 19 in Eqs. 16 and 17.

$$m(\ddot{Z} + \ddot{\alpha}b) = 2\pi\rho aU\Big(-\dot{Z} + U\alpha + \Big(\frac{a}{2} - b\Big)\alpha\Big)C(i\omega) + \pi\rho a^2(-\ddot{Z} + U\dot{\alpha} - b\ddot{\alpha}) + F_a \tag{21}$$

$$J\ddot{\alpha} = -2\pi\rho aU\Big(\frac{a}{2}\Big)^2\dot{\alpha} + \pi\rho a^2U\Big(-\dot{Z} + U\alpha + \Big(\frac{a}{2} - b\Big)\dot{\alpha}\Big) C(i\omega) - \frac{\pi}{8}\rho a^4\ddot{\alpha} + \tau_a - F_a b \tag{22}$$

In this model the forces ($F_a = 127N$, $\tau_a = 10.16N$) are directly transmit from the actuators to the foil. Collecting coefficients of Eqs. 21, 22 and written as;

$$E_1\begin{bmatrix}\ddot{Z}\\ \ddot{\alpha}\end{bmatrix} = E_2\begin{bmatrix}\dot{Z}\\ \dot{\alpha}\end{bmatrix} + E_3T_f + B_0\begin{bmatrix}F_a\\ \tau_a\end{bmatrix} \tag{23}$$

Th coefficient matrix of the Eq. 23 obtained as,

$$E_1 = \begin{bmatrix}m + \pi\rho a^2 & mb + \pi\rho a^2 b\\ 0 & J + \frac{\pi}{8}\rho a^4\end{bmatrix} \tag{24}$$

$$E_2 = \begin{bmatrix}0 & \pi\rho a^2 U\\ 0 & -2\pi\rho\frac{a^3}{4}U\end{bmatrix} \tag{25}$$

$$E_3 = \begin{bmatrix}2\pi\rho aU\\ \pi\rho a^2 U\end{bmatrix} \tag{26}$$

$$B_0 = \begin{bmatrix}127 & 0\\ -127b & 10.16\end{bmatrix} \tag{27}$$

where F_a and τ_a are the control inputs. The common term in both the Eqs. 21 and 22 is $[(\dot{Z} + U\dot{\alpha} + (\frac{a}{2}b)\dot{\alpha})C(i\omega)]$, which taken for the analysis as;

$$T_f(s) = C_f(s)C(s) \tag{28}$$

in which $C(s)$ is the Laplace transform of theodorsen function Eq. 20 by substituting $i\sigma$ as $\frac{as}{U}$. The Theodorsen function treated here as a linear filter in time domain.

$$C(s) = a_c + \frac{a_2s^2 + a_1s + a_0}{s^3 + b_2s^2 + b_1s + b_0} \tag{29}$$

where $a_c = a_3$. From the equation, system is realized to controllable canonical form.

$$\begin{bmatrix}\dot{\phi_{t1}}\\ \dot{\phi_{t2}}\\ \dot{\phi_{t3}}\end{bmatrix} = \begin{bmatrix}0 & 1 & 0\\ 0 & 0 & 1\\ -b_0 & -b_1 & -b_2\end{bmatrix}\begin{bmatrix}\phi_{t1}\\ \phi_{t2}\\ \phi_{t3}\end{bmatrix} + \begin{bmatrix}0\\ 0\\ 1\end{bmatrix}\psi_t$$

$$\gamma = \begin{bmatrix}a_2 - a_3b_2 & a_1 - a_3b_1 & a_3 - a_3b_0\end{bmatrix}\begin{bmatrix}\phi_{t1}\\ \phi_{t2}\\ \phi_{t3}\end{bmatrix} + a_3\psi_t \tag{30}$$

The term in C_f is;

$$C_f = \dot{Z} + U\dot{\alpha} + (\frac{a}{2}b)\dot{\alpha} \tag{31}$$

$$C_f = C_{fk}\begin{bmatrix}Z\\ \alpha\end{bmatrix} + C_{fd}\begin{bmatrix}\dot{Z}\\ \dot{\alpha}\end{bmatrix} \tag{32}$$

where $C_{fk} = \begin{bmatrix}0 & U\end{bmatrix}$ and $C_{fd} = \begin{bmatrix}\frac{a}{b} & -1\end{bmatrix}$.

Let $\phi_t = \begin{bmatrix}\phi_{t1} & \phi_{t2} & \phi_{t3}\end{bmatrix}^T$, $\dot{T_f} = \dot{\phi_t} = \begin{bmatrix}\dot{\phi_{t1}} & \dot{\phi_{t2}} & \dot{\phi_{t3}}\end{bmatrix}^T$, the Eq. 28 will be;

$$\dot{T_f} = \begin{bmatrix}0 & 1 & 0\\ 0 & 0 & 1\\ -b_0 & -b_1 & -b_2\end{bmatrix}\phi_t + \begin{bmatrix}0\\ 0\\ 1\end{bmatrix}C_f = \Phi_{f1}\begin{bmatrix}Z\\ \alpha\end{bmatrix} + \Phi_{f2}\begin{bmatrix}\dot{Z}\\ \dot{\alpha}\end{bmatrix} + \Phi_{f3}\phi t \tag{33}$$

where $\Phi_{f1} = \begin{bmatrix}0 & 0 & 1\end{bmatrix}^T C_{fk}$ and $\Phi_{f2} = \begin{bmatrix}0 & 0 & 1\end{bmatrix}^T C_{fd}$. Substituting realization of T_f in Eq. 23 and solving for $\begin{bmatrix}\ddot{Z} & \ddot{\alpha}\end{bmatrix}^T$;

$$\begin{bmatrix}\ddot{Z}\\ \ddot{\alpha}\end{bmatrix} = F_1\begin{bmatrix}\dot{Z}\\ \dot{\alpha}\end{bmatrix} + F_2\begin{bmatrix}Z\\ \alpha\end{bmatrix} + F_3\phi_t + B_1U_c \tag{34}$$

where $F_1 = E_1^{-1}(E_2 + K_f\phi_{f2})$, $F_2 = E_1^{-1}\phi_{f1}$, $F_3 = E_1^{-1}E_3\phi_{f3}$, $B_1 = E_1^{-1}B_0$ and $U_c = \begin{bmatrix}F_a & \tau_a\end{bmatrix}^T$. Thus the state space representation of the caudal fin system is,

$$\dot{x} = \begin{bmatrix}0_{2x2} & I_{2x2} & 0_{2x3}\\ F_1 & F_2 & F_3\\ \Phi_{f1} & \Phi_{f2} & \Phi_{f3}\end{bmatrix}x + \begin{bmatrix}0_{2x2}\\ B_1\\ 0_{3x2}\end{bmatrix}U_c$$

$$\dot{x} = Ax + BU_c \tag{35}$$

where the system coefficient matrices are A $\epsilon : R^{7\times7}$ and B $\epsilon : R^{7\times2}$. The output equation:

$$Y = \begin{bmatrix}100\ 0\ 0\ 0\ 0\ 0\ 0\\ 0\ \ 2\ 0\ 0\ 0\ 0\ 0\end{bmatrix}x$$

$$y = Cx \tag{36}$$

where the values in the C matrix are the output thrust values ($\tau_X = 100N$ and $\tau_P = 2N$)

3.3 Dorsal fin Dynamics

The hull with dorsal fin vehicle moving in x-y plane, and the coordinates of the center of gravity of the vehicle $[x_g, y_g, z_g] = [0.075, 0, 0]$. The sway and yaw equation of the neutrally buoyant vehicle with dorsal fin is described [28] below:

$$\begin{aligned} I_z\dot{r} + m[x_g(\dot{v} + ur) + y_g vr] &= \frac{\rho}{2}l^5(N_{\dot{r}}\dot{r} + N_{r|\mathrm{r}|}r|\mathrm{r}|) + \frac{\rho}{2}l^4(N_{\dot{v}}\dot{v} + N_{ur}ur) \\ &\quad + \frac{\rho}{2}l^3(N_{uv}uv + N_{v|v|}v|v|) + N_f \\ m(\dot{v} + ur + x_g\dot{r} + y_g r62) &= \frac{\rho}{2}l^4(Y_{\dot{r}}\dot{r} + Y_{r|\mathrm{r}|}r|\mathrm{r}|) + \frac{\rho}{2}l^3(Y_{\dot{v}}\dot{v} + Y_{ur}ur) \\ &\quad + \frac{\rho}{2}l^2(Y_{uv}uv + NY_{v|v|}v|v|) + F_f\dot{\psi} = r \end{aligned} \tag{37}$$

Here v is the sway velocity, ψ is the yaw angle, $F_f = \tau_Y$ and $N_f = \tau_N$ are the net force (sway force) and moment (yaw moment) produced by the dorsal fin. The forward velocity is kept constant by a control mechanism and heave is taken as zero. Nonlinear coefficients are eliminated from the analysis, then the system will be;

$$\begin{bmatrix} (m - \frac{\rho}{2}l^3Y_{\dot{v}}) & (mx_g - \frac{\rho}{2}l^4Y_{\dot{r}}) \\ (mx_g - \frac{\rho}{2}l^4N_{\dot{v}}) & (I_z - \frac{\rho}{2}l^5N_{\dot{r}}) \end{bmatrix}\begin{bmatrix}\dot{v}\\ \dot{r}\end{bmatrix} + \begin{bmatrix} mur \\ mx_g u\end{bmatrix}\begin{bmatrix}v\\ r\end{bmatrix} = \begin{bmatrix}\tau_Y\\ \tau_N\end{bmatrix} \tag{38}$$

The Eq. 38 written as,

$$\begin{aligned} \begin{bmatrix}\dot{v}\\ \dot{r}\end{bmatrix} = &-\begin{bmatrix} (m - \frac{\rho}{2}l^3Y_{\dot{v}}) & (mx_g - \frac{\rho}{2}l^4Y_{\dot{r}}) \\ (mx_g - \frac{\rho}{2}l^4N_{\dot{v}}) & (I_z - \frac{\rho}{2}l^5N_{\dot{r}}) \end{bmatrix}^{-1}\begin{bmatrix} mur \\ mx_g u\end{bmatrix}\begin{bmatrix}v\\ r\end{bmatrix} \\ &+\begin{bmatrix} (m - \frac{\rho}{2}l^3Y_{\dot{v}}) & (mx_g - \frac{\rho}{2}l^4Y_{\dot{r}}) \\ (mx_g - \frac{\rho}{2}l^4N_{\dot{v}}) & (I_z - \frac{\rho}{2}l^5N_{\dot{r}}) \end{bmatrix}^{-1}\begin{bmatrix}\tau_Y\\ \tau_N\end{bmatrix} \end{aligned} \tag{39}$$

This equation of the form of state space representation, $\dot{x} = Ax + Bu$ and the output equation will be,

$$y = \begin{bmatrix}40 & 0.4\end{bmatrix}\begin{bmatrix}v\\ r\end{bmatrix} \tag{40}$$

3.4 Pectoral fin Dynamics

The hull with pectoral fin vehicle moving in x-z plane, and the coordinates of the center of gravity of the vehicle $[x_g, y_g, z_g] = [0.075, 0, 0]$. The heave and pitch equation of the neutrally buoyant vehicle with dorsal fin is described [28] below:

$$\begin{aligned} m[\dot{w} - uq - x_g\dot{q} - z_g q^2] &= Z_{\dot{q}}\dot{q} + Z_{\dot{w}}\dot{w} + Z_{uq}uq \\ &\quad + Z_{uw}uw + F_p \\ I_y\dot{q} - m[x_g(\dot{w} - uq) - z_g wq] &= M_{\dot{q}}\dot{q} + M_{\dot{w}}\dot{w} + M_{uq}uq \\ &\quad + M_p - x_{gb}Wcos\theta \\ &\quad - z_{gb}Wsin\theta] \\ \dot{\theta} &= q \\ \dot{z} &= w - u\theta \end{aligned} \tag{41}$$

Here w is the heave velocity, θ is the pitch angle, $F_p = \tau_Z$ and $M_p = \tau_M$ are the net force (heave thrust) and moment (pitch moment) produced by the pectoral fin. The forward velocity is kept constant by a control mechanism and for simplicity nonlinear coefficients are eliminated, then the system will be;

$$\begin{bmatrix} (m - Z_{\dot{w}}) & (mx_g - Z_{\dot{q}}) \\ (-mx_g - M_{\dot{w}}) & (I_y - M_{\dot{q}}) \end{bmatrix}\begin{bmatrix}\dot{w}\\ \dot{q}\end{bmatrix} = \begin{bmatrix} Z_w U & Z_q + mU \\ M_w U & M_q - mx_g U\end{bmatrix}\begin{bmatrix}w\\ q\end{bmatrix} + \begin{bmatrix}\tau_Z\\ \tau_M\end{bmatrix} \tag{42}$$

Re-writing the Eq. 41,

$$\begin{aligned} \begin{bmatrix}\dot{w}\\ \dot{q}\end{bmatrix} = &\begin{bmatrix} (m - Z_{\dot{w}}) & (mx_g - Z_{\dot{q}}) \\ (-mx_g - M_{\dot{w}}) & (I_y - M_{\dot{q}}) \end{bmatrix}^{-1}\begin{bmatrix} Z_w U & Z_q + mU \\ M_w U & M_q - mx_g U\end{bmatrix}\begin{bmatrix}w\\ q\end{bmatrix} \\ &+\begin{bmatrix} (m - Z_{\dot{w}}) & (mx_g - Z_{\dot{q}}) \\ (-mx_g - M_{\dot{w}}) & (I_y - M_{\dot{q}}) \end{bmatrix}^{-1}\begin{bmatrix}\tau_Z\\ \tau_M\end{bmatrix} \end{aligned} \tag{43}$$

This equation of the form of state space representation, $\dot{x} = Ax + Bu$ and the output equation will be,

$$y = \begin{bmatrix}50 & 1\end{bmatrix}\begin{bmatrix}w\\ q\end{bmatrix} \tag{44}$$

3.5 Representation of Biomimetic AUV System

The inputs given to the caudal fin are force and torque, from the motor actuator. Due to the motions of the fin it can produce the forward thrust ($\tau_X = 100N$) and the angular moment which are used as the input to the AUV hull subsystem. Caudal fin and hull subsystem are taken as a cascade connection, and the pectoral fin subsystem and dorsal fin subsystem are connected parallel to this. The inputs to the pectoral fin are heave thrust and pitch moment where as output from this system are heave and pitch velocities. Similarly, the inputs to the dorsal fin are sway thrust and yaw moment where as output from this system are sway and heave velocities. The whole system is subjected

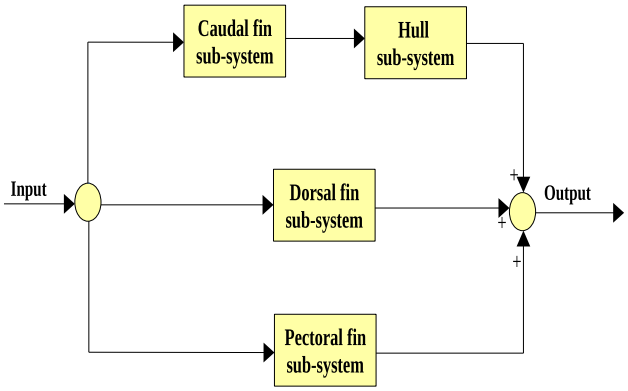

Fig. 6 Block diagram model of the Biomimetic AUV system

to the control applications such as velocity control, depth -pitch control, heading, roll, and trajectory tracking. The Fig. 6 shows the block diagram representation of the coupled Biomimetic AUV system and Fig. 7 illustrated the MATLAB/Simulink model of the system.

The thrust values of the proposed system is illustrated in the Table 2.

3.6 Disturbance Effect

Two different disturbance effects are taken for the system analysis: ocean current and wave disturbance.

Table 2 Thrust values of Biomimetic AUV system

Forces/ Moments	Values
τ_X	100 N
τ_Y (F_f)	40 N
τ_Z (F_p)	50 N
τ_K	2 Nm
τ_M (M_P)	1 Nm
τ_N (N_f)	0.4 Nm

Ocean current disturbance The ocean currents can be assumed to be the primary disturbance for the AUVs. These effects are horizontal and vertical circulation systems of ocean waters created by gravity, wind friction, and water density change in different ocean areas [10]. The equation of motion of ocean currents can be represented in in terms of relative velocity v_r [10] as,

$$v_r = V - V_c \tag{45}$$

where $V_c = \begin{bmatrix} u_c & v_c & w_c & 0 & 0 & 0 \end{bmatrix}^\top$ is the ocean current velocity vector, considering that the current does not generate rotational movement on the vehicle. In the present assessment, velocity of the ocean current ranges from $(0 - 4m/s)$ has been taken (Table 3).

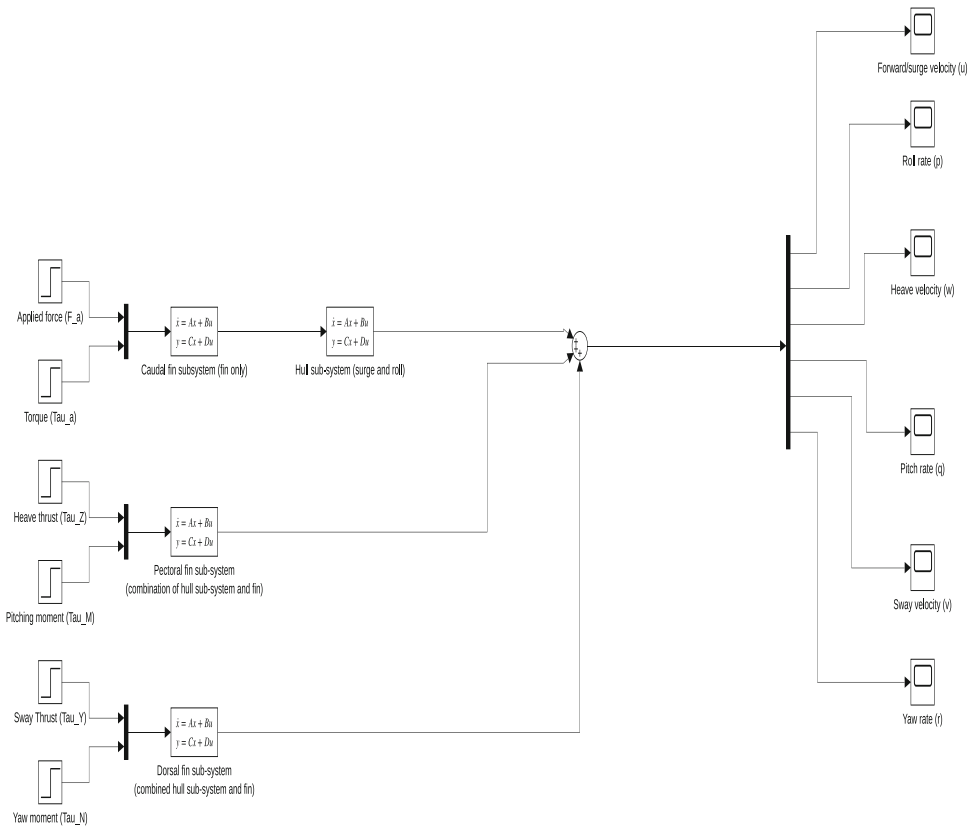

Fig. 7 Simulink model of the Biomimetic AUV system

Table 3 Disturbance wave parameters [29]

Wave height	4.1 m
Wave length	77 m
ω_0	0.7302 rad/s
σ	1639.98 W/m^2

Wave disturbance When an AUV approaches the sea surface, it also experiences wave disturbance. In this study, the following Wave transfer function [9, 29] is defined:

$$h(s) = \frac{K_\omega}{s^2 + 2\lambda\omega_0 s + \omega_0^2} \tag{46}$$

where λ is damping coefficient and ω_0 is dominating wave frequency, and $K_\omega = 2\lambda\omega_0\sigma$ with σ as the wave intensity. Here the wave is considering with following parameters such as;

Due to the large waves, heavy rolling and pitching may occur to the underwater vehicle. That causes damage to the hull and equipment inside. So heave and roll control are also introduced [29] for the coupled biomimetic AUV system, which eliminates these effects, thus avoiding breach impairment.

4 Stability Analysis of the Coupled System

Stability analysis for the underwater vehicle is defined as its ability to restore to the equilibrium state after being disrupted without requiring any corrective action. Nevertheless, stability and adequate performance cannot be assured since the systems are effectively [30] coupled. In order to verify the suggested model, an underwater stability investigation is performed which posses the following steps in Fig. 8.

4.1 Stability Analysis of Caudal fin sub System

The caudal fin subsystem of proposed AUV is a Multi - Input - Multi - Output (MIMO) system with two inputs and outputs. For the caudal fin system, linear time-invariant continuous-time MIMO systems with proper square transfer matrix $Gcfin(s) \in R^{m\times m}(s)$ is considered. Alternatively, the systems defined in state-space representation as:

$$\begin{aligned} \dot{x} &= Ax + BU_c \\ y &= Cx + DU_c \end{aligned} \tag{47}$$

where $x \in \mathbb{R}^n$, $u \in \mathbb{R}^m$, $y \in \mathbb{R}^m$, $A \in \mathbb{R}^{n\times n}$, $B \in \mathbb{R}^{n\times m}$, $C \in \mathbb{R}^{m\times n}$, $D \in \mathbb{R}^{m\times m}$, and the transfer matrix is given by $Gcfin(s) = C(sI - A)^{-1}B + D$ $(D = 0)$. The system $Gcfin(s)$ will be;

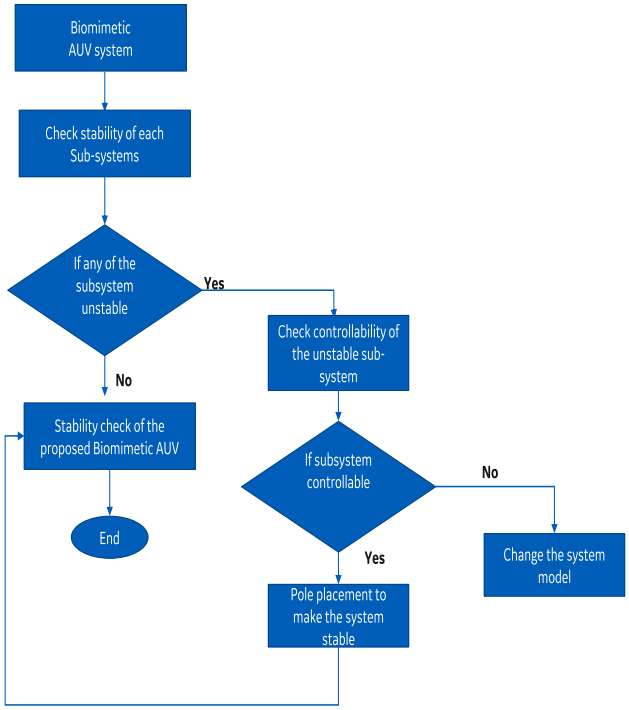

Fig. 8 Flow chart of the stability analysis

$$Gcfin(s) = \begin{bmatrix} Gcfin_1(s) & Gcfin_2(s) \\ Gcfin_3(s) & Gcfin_4(s) \end{bmatrix} \tag{48}$$

The Bode plot of system is shown in Fig. 9.

The phase margin (PM) in the bode plot for $Gcfin_4(s)$ is $-180°$, and some poles of the system lies in right half of s-plane. Hence it is clear that the caudal fin system is unstable.

4.2 Controllability of Caudal fin Subsystem

A system is considered entirely controllable if, upon receiving a controlled input, it can transition from its original state to any desired state in a finite amount of time. The subsystem of the caudal fin is represented by the Eq. 47, where $x \in \mathbb{R}^n$ is the internal state of the system and U_c is an input signal applied to one of the system's units. The dimensions of the factors A and B are 7×7 and 7×2, respectively. The matrices A and B vary in time, the concept of controllability is tied to a specific, finite time interval denoted $[t_0, t_f]$ with $t_f > t_0$. The linear state Eq. 52 is controllable on $[t_0, t_f]$ if given any initial state $x(t_0) = x_0$ there exists a continuous input signal $u(t)$ such that the corresponding solution of Eq. 47 satisfies $x(t_f) = 0$. The

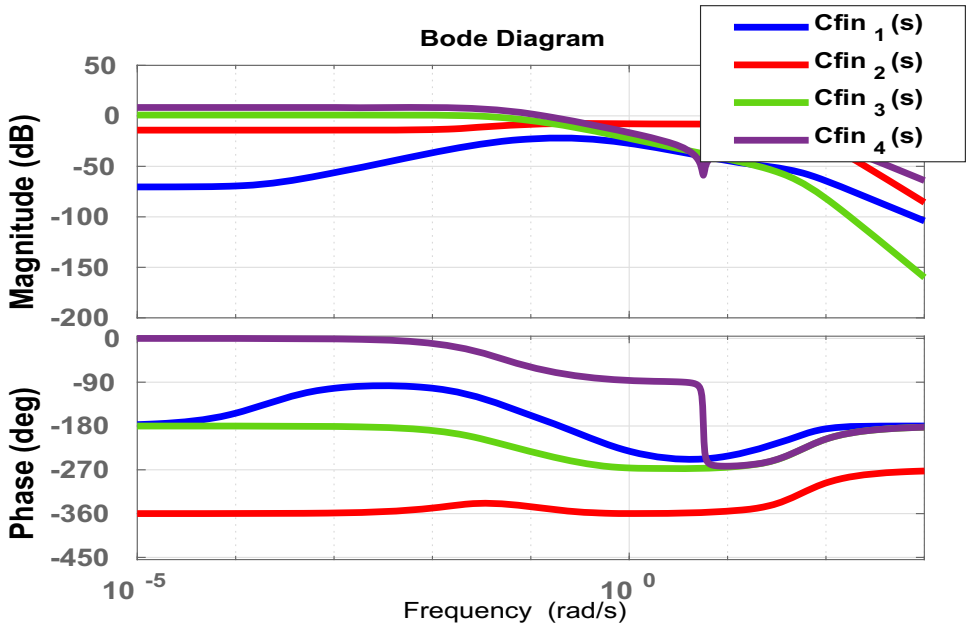

Fig. 9 MIMO Bode plot of caudal fin subsystem

caudal fin subsystem Eq. 47 is controllable, if and only if controllability matrix has full rank.

$$Co = \begin{bmatrix} B & AB & A^2B & A^3B & A^4B & A^5B & A^6B \end{bmatrix} \tag{49}$$

In this proposed system,

$$rank(Co) = 7 \tag{50}$$

From the Eq. 50 found that the system is completely state controllable.

4.2.1 Design Using Pole Placement

The pole placement is a technique used in the theory of feedback control systems to position the closed-loop poles of a plant at predetermined positions in the s-plane. The placement of poles is beneficial because the location of the poles corresponds directly to the system eigenvalues, which govern the system response characteristics. The system must be considered controllable for this method to be implemented. Full state feedback is utilized by commanding the input vector Eq. 47 U_c. Consider an input proportional (in the matrix sense) to the state vector,

$$U_c = Kx \tag{51}$$

Substituting this into Eq. 47;

$$\begin{aligned} \dot{x} &= (A - BK)x \\ y &= (C - DK)x \end{aligned} \tag{52}$$

The poles of the system are given by the characteristic equation of the matrix $A - BK$, $det[sI - (A - BK)] = 0$. Comparing the elements of this equation to those of the desired characteristic equation produces the feedback matrix K values that drive the closed-loop eigenvalues to the pole positions indicated by the desired characteristic equation(Fig. 10).

4.3 Biomimetic AUV Coupled System Stability Analysis

The coupled Biomimetic AUV system is a MIMO system with seven inputs and outputs, and the state space representation is;

$$\begin{aligned} \dot{x_{BAUV}} &= A_{BAUV}x + B_{BAUV}u \\ y_{BAUV} &= C_{BAUV}x + D_{BAUV}u \end{aligned} \tag{53}$$

The coupled system is linear and Lyapunov direct method is used for the stability analysis. Consider a linear autonomous system

$$\dot{X} = AX \tag{54}$$

The system is stable when;

Theorem 1 *For $A \in \mathbb{R}^{n\times n}$ the following statements* [31] *are equivalent:*

1. *A is Hurwitz*
2. *For all $Q = Q^T > 0$ there exists a unique $P = P^T > 0$ satisfying the Lyapunov equation*

$$A^T P + PA = -Q \tag{55}$$

where P and Q matrices are determined by using LMI (Linear Matrix Inequalities) method. So the proposed system will be stable with the conditions such that;

$$A_{BAUV}^T P + PA_{BAUV} = -Q \tag{56}$$

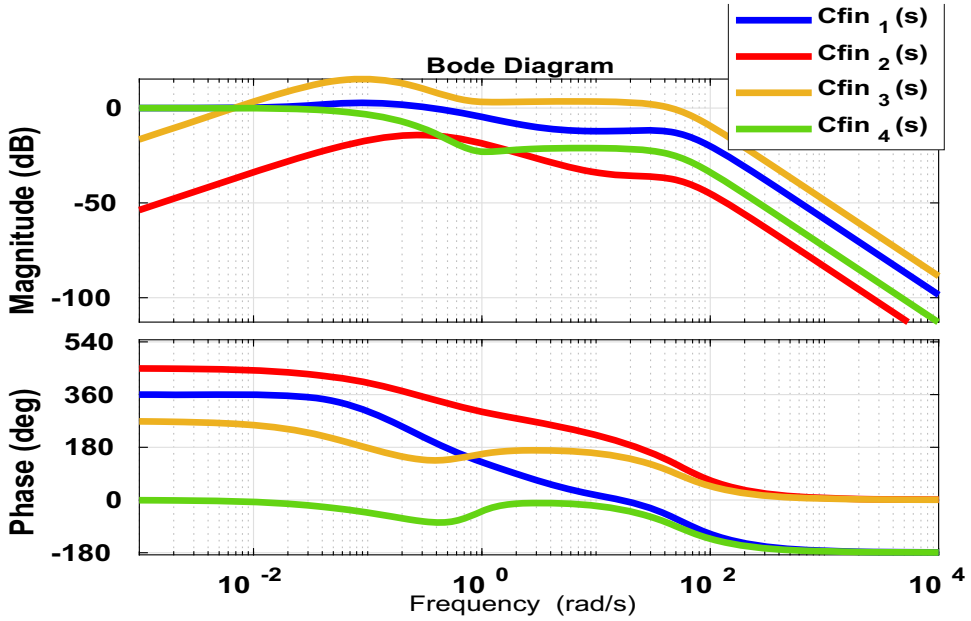

Fig. 10 MIMO bode plot for stable caudal fin subsystem

5 Stress Assessment of Biomimetic AUV System

Stress test of the submerged structures, especially for AUVs, is a crucial step to building a design of an underwater vehicle. It can be done by using different methods such as analytical calculation, finite element analysis etc. The shape and material of the vehicle play an important role in stress analysis. Aluminum and Titanium alloy are widely used in AUVs because they possess light weight, high strength, and high corrosion resistance [32].

Static and dynamic loading are two types of loads that typically affect remotely driven vehicles. Due to the weight of the water column above the vehicle and adherence to the well-known rule:

$$P_s = \rho g h \tag{57}$$

where P_s is the static pressure, g is the acceleration due to gravity, h is the height of the water column above vehicle and ρ is the water density. Let h assumed to be as $40m$ [16], $P_s = 1000 \times 9.81 \times 40 = 0.392 MPa$. The dynamic loading causes dynamic stress, which is due to the speed of the vehicle. This stress obeys Bernoulli's equation,

$$P_d = \frac{1}{2}\rho v^2 \tag{58}$$

where P_d is the dynamic pressure, v is the velocity and ρ is the water density. The velocity of the vehicle is taken as $2.57 m/s$ [16]. Therefore the calculated P_d will be, $P_d = \frac{1}{2} \times 1000 \times 2.57 = 3.302 KPa$.

5.1 Stress Calculation of Different Parts

In the present issue, analytical calculation method is used for the stress analysis of AUV structure. The dynamic pressure is lower for the vehicle than the static pressure, so the dynamic load due to vehicle velocity can be neglected.

- AUV hull : The dimensional parameters of the hull already defined in Table 1. The total stress obtained for this geometry is $47.62 MPa$.
- Caudal fin : The dimensional parameters of the caudal fin is illustrated in Table 4.
  The stress obtained for the caudal fin is $3.15 MPa$.
- Dorsal fin: The design parameters for the dorsal fin is described in Table 5 and the stress calculated for this is $0.63 MPa$.
- Pectoral fin: The stress calculation of pectoral fin also like the similar way of the other fins. All the dimensional parameters are delineated in Table 6 and the stress procured is $0.68 MPa$.

Table 4 Dimension parameters of the caudal fin

Flapping foil specifications	
Chord	0.16m
Breadth	0.2285m
Maximum thickness	0.03427m
Area	0.0757 m^2
Maximum frequency	5.27 Hz

Table 5 Dimension parameters of the Dorsal fin

Dorsal fin specifications	
Chord	0.0796m
Breadth	0.1592m
Maximum thickness	9.5588×10^{-3}m
Maximum frequency	6 Hz

6 Coupled Biomimetic AUV System Control

The coupled model of Biomimetic AUV is validated by designing a velocity, roll and pitch controller using PID control. A proportional – integral – derivative controller (PID controller or three-term controller) is a control loop mechanism employing feedback that is widely used in industrial control systems and a variety of other applications requiring continuously modulated control [33]. The time domain output of a PID controller $y(t)$, is calculated from the feedback error denoted as $e(t)$ as follows;

$$y(t) = K_p e(t) + K_i \int e(t)dt + K_d \frac{de(t)}{dt} \tag{59}$$

where K_p, K_i and K_d are the controller gains. Different tuning methods such as manual tuning, zieglar - nichols method, cohen - coon method, genetic algorithm, PSO, etc, can be used to find out these controller gains.

6.1 PID Controller Based Velocity Tracking

PID controller based system can track the desired surge velocity [11] of the proposed AUV. A genetic algorithm based tuning method is used here to find out the controller gains of proposed system. Genetic algorithm is a heuristically designed evolutionary algorithm (EA) [16], [11] inspired by natural selection [34]. The input to the system is applied force (F_a) / torque (τ_a) and output is surge velocity (u). Figure 11 shows the coupled velocity tracking system of Biomimetic AUV.

Here, the procured equation from Eq. 59 for the velocity tracking controller will be:

$$y(t) = 2.8879e(t) + 3.0501 \int e(t)dt + 10.0419 \frac{de(t)}{dt} \tag{60}$$

Table 6 Dimension parameters of the pectoral fin

Pectoral fin specifications	
Chord	0.0718m
Breadth	0.0976m
Maximum thickness	0.01197m
Maximum frequency	8 Hz

When the vehicle is subjected to an ocean current disturbance, the output equation for the velocity tracking controller will be:

$$y(t) = 5.789e(t) + 0.161 \int e(t)dt + 17.516 \frac{de(t)}{dt} \tag{61}$$

6.2 PID Controller Based roll and Pitch Tracking

Roll is a tilting motion of an underwater vehicle from side to side, so that it is an unwanted motion. Similarly, pitch is a rotational up-down motion along the Y axis. The effect of these two motions is taken into account only when the vehicle subjected to wave. The obtained PID controller equations for roll and pitch control is given below:

- **Case I:** Roll system with wave disturbance

$$y(t) = 78.35e(t) + 0.249 \int e(t)dt + 131.53 \frac{de(t)}{dt} \tag{62}$$

- **Case II:** Pitch system with wave disturbance

$$y(t) = 11.789e(t) + 4.04 \int e(t)dt + 23.83 \frac{de(t)}{dt} \tag{63}$$

7 Results and Discussion

The proposed dynamic model of the Biomimetic AUV has been designed using state space formulation method. The dynamic equation of each part of the vehicle is modeled separately and coupled all these parts (virtual) together to get the final model.

One of the most critical aspects of the control quality of an autonomous underwater vehicle is the stability of the motion control system. The stability analysis has been performed using Lyapunov direct method. The proposed system is satisfying Lyapunov Eq. 56. Figure 12 shows the bode plot of the Biomimetic AUV system.

The gain margin and phase margin of the system are positive. So it is clear from this plot that the system is stable.

7.1 Stress Analysis of Biomimetic AUV

The stresses of the individual part of the vehicle have been calculated, and the total stress attained is $52.08 MPa$. Aluminum or titanium alloy are commonly used to build underwater vehicles. The present value is computed for the vehicle composed of aluminum alloy, which will also come under the range of titanium alloy. The maximum permissible stress values range from ($240 MPa$ to $1400 MPa$), and titanium alloy will be ($240 MPa$ - $1400 MPa$). The premeditated underwater vehicle stress value is less than the maximum stress range of the construction materials.

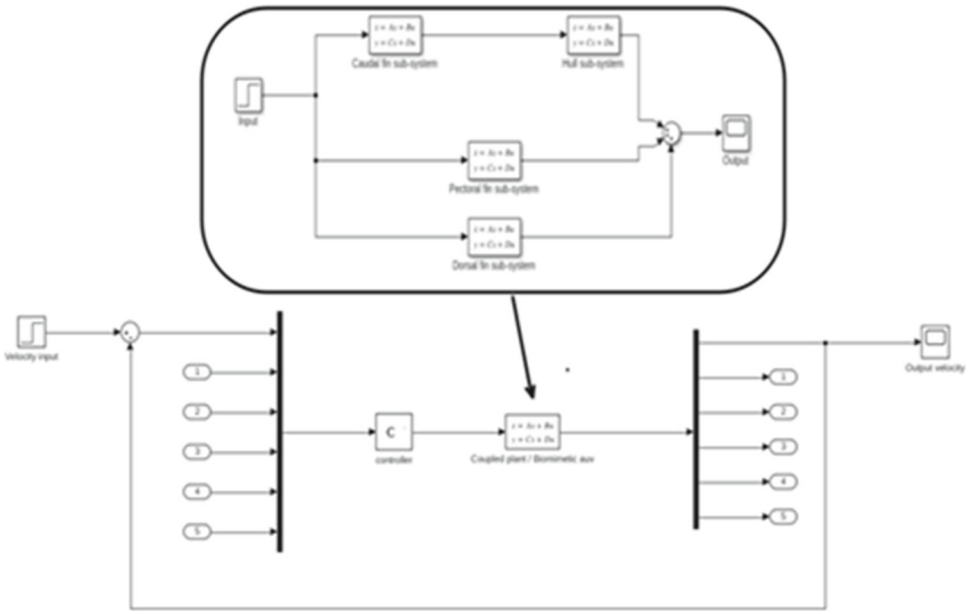

Fig. 11 Block diagram of coupled velocity tracking control

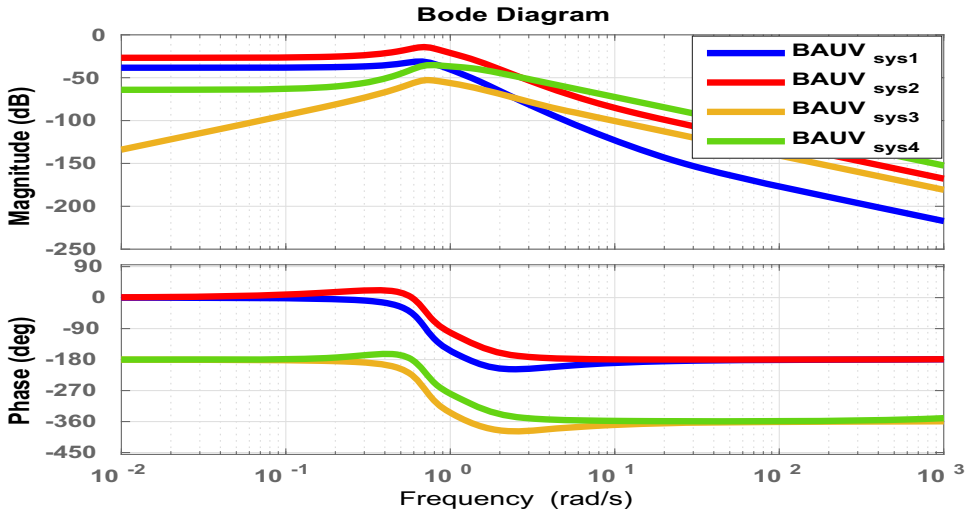

Fig. 12 Bode plot for stable Biomimetic AUV system

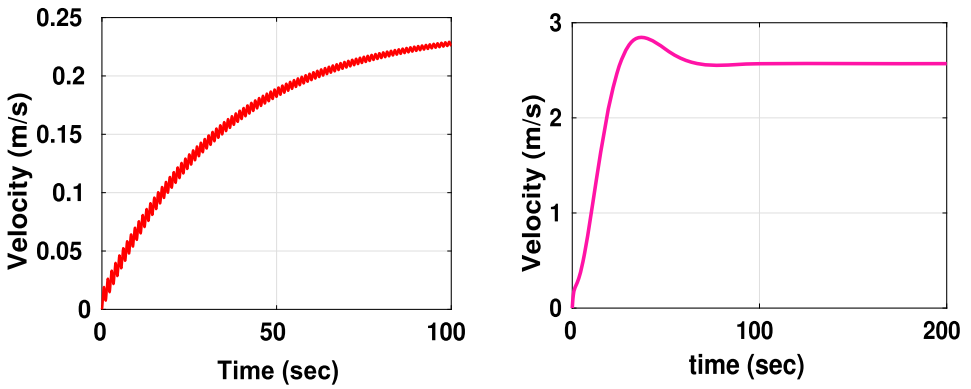

Fig. 13 Velocity tracking response of biomimetic AUV without disturbance

(a) Open-loop velocity response

(b) Coupled velocity tracking system

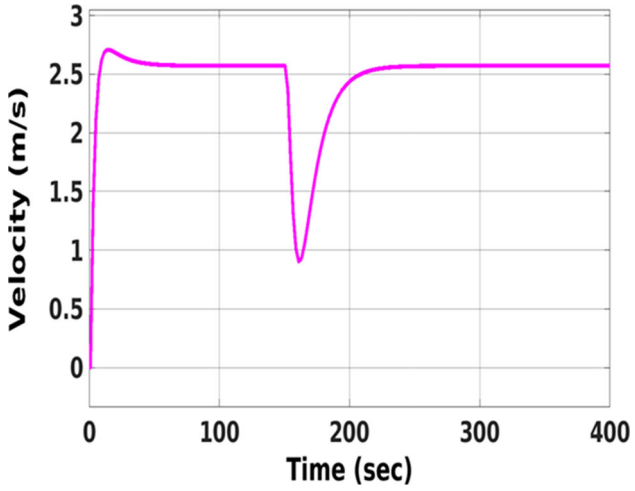

Fig. 14 Coupled velocity tracking system with ocean current disturbance

Effect of disturbances on the vehicle stress Since the ocean current is nothing but a relative velocity, as speed rises, so does the stress on the vehicle. The ocean wave effects include modifying the underwater vehicle structural force, dynamics, and movement. Thus it leads to a rise in the total stress of the vehicle. However, the maximum change in stress is $(30MPa - 50MPa)$ for both disturbance cases. This rise in stress is still within the tolerance range.

Constraints of BAUV stress testing The factors that affect the stress analysis of AUV are material selection, depth at which the vehicle is below the sea surface, shape, and wall thickness. Since most AUVs are made of metal or metal alloy, they can withstand a certain amount of stress before buckling or collapsing. So the selection of material acts as a constraint in the stress analysis. Similarly, increasing the hydrostatic pressure upsurge the depth of the

Fig. 15 Roll system response of biomimetic AUV with ocean current disturbance

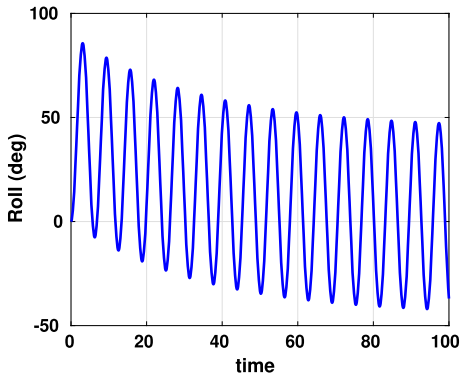

(a) Open-loop roll system response

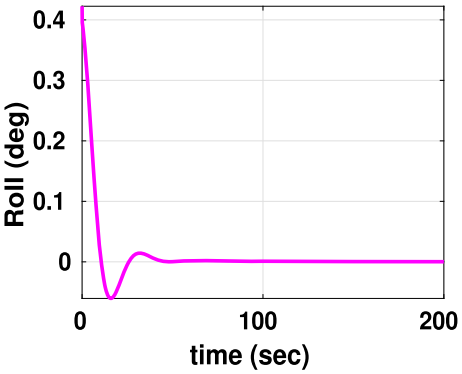

(b) Closed-loop (controlled) roll system response

Fig. 16 Pitch system response of biomimetic AUV with ocean current disturbance

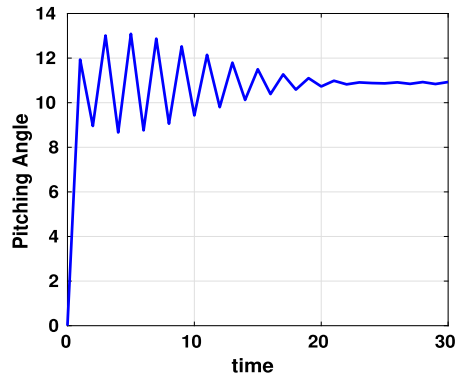

(a) Open-loop pitch system response

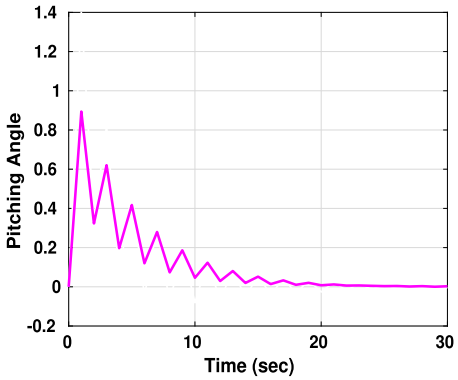

(b) Closed-loop (controlled) pitch system response

submarine and thus increases stress. This stress then strains the hull. Wall thickness also depends on the stress; the radial stress decreases as the thickness increases. However, thickness ought to be considered appropriate. Otherwise, the jumboized equipment would not have sufficient room inside the hull. Thus, the appropriate selection of all these limiting factors is needed to develop a practical biomimetic underwater vehicle design.

7.2 Coupled System Responses

The designed mathematical model of the biomimetic AUV is validated by taking different controlled response conditions such as velocity control response without disturbance, with ocean current disturbance, roll response and heave response.

For the velocity tracking without disturbance case, the system is implemented based on the change of speed, which prompts identical movement conditions. Figure 13a shows the open-loop velocity response and Fig. 13b describes the coupled system velocity tracking response (controlled response) using PID controller.

The ocean current disturbance (velocity in between $(0.1m/s$ - $4m/s)$ is added to the controlled response at a particular time (say 150s) and modeled the controller to remove this. The system reached to steady state (after $70s$) by rejecting the disturbance shown in Fig. 14.

The influence of rolling and pitching can be neglected when the AUV is under water. As mentioned earlier, the ocean current does not produce any rotational movements to the vehicle. In the case of roll and pitch controller;

- Case I : Roll system with ocean current disturbance.

The open-loop response and the controlled response of roll system with presence of wave disturbance shown in Fig. 15a and b.

- Case II : Pitch system with ocean current disturbance.

The open-loop response and the controlled response of pitch system with presence of wave disturbance shown in Fig. 16a and b.

8 Conclusion

This study has described the development of dynamic model of the Biomimetic underwater vehicle. State space formulation method is used here to create the appropriate model. The vehicle is modeled with conventional dynamic equations of Fossen ([9, 10]) with several modifications. The stability analysis has been performed to endorse the model for and found that the system is completely state controllable and stable. In order to validate the model capability, a coupled velocity tracking system, roll and pitch control system with disturbance effect is designed.

Acknowledgments The author gratefully acknowledges Dr. P Anantha krishnan, Department of Ocean Engineering, Indian Institute of Technology, Madras for his valuable support and cooperation to do this research.

Author Contributions The author contributed to the conception and design of this study. Material preparation, analysis, and implementation were performed by Aruna M V.

Declarations

Conflict of Interests The authors declare that there is no conflict of interest.

References

1. Puthenkalathil, R.C.: Unraveling the mechanism of biomimetic hydrogen fuel production. PhD thesis University of Amsterdam (2021)
2. Purpose, S.: Underwater Research Vehicle (SPURV) (2016)
3. Widditsch, H.: Spurv-The First Decade. Technical report, WASHINGTON UNIV SEATTLE APPLIED PHYSICS LAB (1973)
4. Gertler, M., Hagen, G.R.: Standard Equations of Motion for Submarine Simulation. Technical report, David w Taylor Naval Ship Research and Development Center Bethesda MD (1967)
5. Feldman, J.: Dtnsrdc Revised Standarrd Submarine Equations of Motion. Technical report, DAVID W TAYLOR NAVAL SHIP RESEARCH AND DEVELOPMENT CENTER BETHESDA MD SHIP.. (1979)
6. Schindele, D., Aschemann, H.: P-type ilc with phase lead compensation for a pneumatically driven parallel robot. In: 2012 American Control Conference (ACC), pp. 5484–5489. IEEE (2012)
7. Humphreys, D.: Development of the Equations of Motion and Transfer Functions for Underwater Vehicles. Technical report, NAVAL COASTAL SYSTEMS LAB PANAMA CITY FLA (1976)
8. Nahon, M.: A simplified dynamics model for autonomous underwater vehicles. In: Proceedings of Symposium on Autonomous Underwater Vehicle Technology, pp. 373–379. IEEE (1996)
9. Fossen, T.I.: Guidance and control of ocean vehicle. Wiley (1994)
10. Fossen, T.I.: Handbook of marine craft hydrodynamics and motion control. Wiley (2011)
11. Aruna, M.: Heading and obstacle avoidance of biomimetic auv using advanced control strategies. In: OCEANS 2022-Chennai, pp. 1–7. IEEE (2022)
12. Saout, O.: Computation of Hydrodynamic Coefficients and Determination of Dynamic Stability Characteristics of an Underwater Vehicle including Free Surface Effects. PhD thesis, Florida Atlantic University (2003)
13. Gertler, M.: A Reanalysis of the Original Test Data for the Taylor Standard Series. Technical report, DAVID TAYLOR MODEL BASIN WASHINGTON DC (1954)
14. Saout, O., Ananthakrishnan, P.: Hydrodynamic and dynamic analysis to determine the directional stability of an underwater vehicle near a free surface. Appl. Ocean Res. **33**(2), 158–167 (2011)
15. V, A.M.: A Virtual Design and Simulation of Biomimetic Autonomous Underwater Vehicle. unpublished manuscript (2021)

16. Aruna, M.: Velocity tracking and pitch depth regulation of biomimetic autonomous underwater vehicle using different control strategies. In: International Journal of Vehicle Autonomous Systems, (Under Review) (2022)
17. Ahmad Mazlan, A.N.: A Fully Actuated Tail Propulsion System for a Biomimetic Autonomous Underwater Vehicle. PhD thesis, University of Glasgow (2015)
18. Triantafyllou, M.S., Techet, A.H., Hover, F.S.: Review of experimental work in biomimetic foils. IEEE J. Ocean. Eng. **29**(3), 585–594 (2004)
19. Lighthill, M.J.: Aquatic animal propulsion of high hydromechanical efficiency. J. Fluid Mech. **44**(2), 265–301 (1970)
20. von Karman, T.H., Sears, W.R.: Airfoil theory for non-uniform motion. J. Aeronaut. Sci. **5**(10), 379–390 (1938)
21. Kanat, Ö.Ö., Karatay, E., Köse, O., Oktay, T.: Combined active flow and flight control systems design for morphing unmanned aerial vehicles. Proceedings of the Institution of Mechanical Engineers, Part G: Journal of Aerospace Engineering **233**(14), 5393–5402 (2019)
22. Kose, O., Oktay, T.: Simultaneous quadrotor autopilot system and collective morphing system design. Aircr. Eng. Aerosp. Technol. **92**(7), 1093–1100 (2020)
23. Oktay, T., Coban, S.: Simultaneous longitudinal and lateral flight control systems design for both passive and active morphing tuavs. Elektronika ir elektrotechnika **23**(5), 15–20 (2017)
24. Licht, S., Hover, F., Triantafyllou, M.S.: Design of a flapping foil underwater vehicle. In: Proceedings of the 2004 International Symposium on Underwater Technology (IEEE Cat. No. 04EX869), pp. 311–316. IEEE (2004)
25. Theodorsen, T., Mutchler, W.: General theory of aerodynamic instability and the mechanism of flutter (1935)
26. Harper, K.A., Berkemeier, M.D., Grace, S.: Modeling the dynamics of spring-driven oscillating-foil propulsion. IEEE J. Ocean. Eng. **23**(3), 285–296 (1998)
27. Singh, S.N., Mani, S.: Control of oscillating foil for propulsion of biorobotic autonomous underwater vehicle (auv). Appl. Bionics Biomech. **2**(2), 117–123 (2005)
28. Narasimhan, M.: Dorsal and pectoral fin control of a biorobotic autonomous underwater vehicle. University of Nevada, Las Vegas (2005)
29. Aruna, M.: Heave and roll control of biomimetic autonomous underwater vehicle using distinct control methods. In: OCEANS 2022-Hampton Roads (2022)
30. Elnashar, G.A.: Performance and stability analysis of an autonomous underwater vehicle guidance and control. In: 2013 5th International Conference on Modelling, Identification and Control (ICMIC), pp. 67–73. IEEE (2013)
31. Sastry, S.: Lyapunov stability theory. In: Nonlinear Systems, pp. 182–234. Springer (1999)
32. Badawy, A., Omer, A.: Stress and dynamic analysis of simple remotely operated underwater vehicle. In: The International Conference on Applied Mechanics and Mechanical Engineering, vol. 15, pp. 1–22 (2012). Military Technical College
33. Bennett, S.: Development of the pid controller. IEEE Control. Syst. Mag. **13**(6), 58–62 (1993)
34. Thomas, N., Poongodi, D.P.: Position control of Dc motor using genetic algorithm based Pid controller. In: Proceedings of the World Congress on Engineering, vol. 2, pp. 1–3, London, UK (2009)

Aruna M V is a research scholar in the Department of Ocean Engineering, Indian Institute of Technology - Madras, India since 2017. She holds a master (2016) and bachelor's (2013) degree from University of Calicut - Kerala, India. Her current research interests include the dynamics and control of underwater vehicle, optimization and AI/ML algorithms. She is having a multidisciplinary background in the areas of biomedical instrumentation, data science, ocean engineering, electronics and process control.